Microbiology Papers in Press. Published June 3, 2010 as doi:10.1099/mic.0.039719-0

Selenite-induced cell death in *Saccharomyces cerevisiae*: protective role of glutaredoxins

Alicia Izquierdo, Celia Casas and Enrique Herrero*

Departament de Ciències Mèdiques Bàsiques, IRBLleida, Universitat de Lleida, Montserrat Roig 2, 25008-Lleida, Spain

Running title: Selenite-induced death in yeast and glutaredoxins role

Contents category: Cell and Molecular Biology of Microbes

*Corresponding author. Phone +34 973 702409; Fax +34 973 702426; E-mail: enric.herrero@cmb.udl.cat

Abreviations: AIF, Apoptosis-inducing Factor; DAPI, 4,8-diamidino-2-phenylindole; DNPH, dinitrophenylhydrazine; GRX, glutaredoxin; GSH, reduced glutathione; PBS, phosphate-buffered saline; ROS, reactive oxygen species

SUMMARY

In contrast to higher organisms, selenium is not essential for growth in *Saccharomyces cerevisiae*. In this species, it causes toxic effects at high concentrations. In the present study, we show that when supplied as selenite to yeast cultures growing under fermentative metabolism, its effects can be dissected into two death phases. From initial treatment times, it causes loss of membrane integrity and genotoxicity. Both effects occur at higher levels in mutants lacking Grx1p and Grx2p than in wild type cells, and are reversed by expression of a cytosolic version of the membrane-associated Grx7p glutaredoxin. Grx7p can also rescue the high levels of protein carbonylation damage occurring in selenite-treated cultures of the *grx1 grx2* mutant. At advances times, selenite causes abnormal nuclear morphology and appearance of TUNEL-positive cells, which are considered apoptotic markers in yeast cells. This effect is independent of Grx1p and Grx2p. Therefore, the protective role of both glutaredoxins is circumscribed to the initial stages of selenite treatment. Lack of Yca1p metacaspase or of a functional mitochondrial electron transport chain only moderately diminishes apoptotic-like death by selenite. In contrast, selenite-induced apoptosis is dependent on the apoptosis-inducing factor Aif1p. In the absence of the latter, intracellular protein carbonylation is reduced after prolonged selenite treatment, supporting that part of the oxidative damage is contributed by apoptotic cells.

INTRODUCTION

Selenium (Se) is a trace element which may have anticarcinogenic action at low concentrations (Letavayová *et al*., 2006). The dietary essential character of Se in mammals is related to its presence as selenocysteine in a number of selenoproteins, such as thioredoxin reductases and glutathione peroxidases (Lu & Holmgren, 2009). These enzymes act in the defence against oxidative stress. In contrast, at high concentrations Se is toxic because it generates oxidative stress and provokes DNA damage (Hatfield *et al*., 2006; Letavayová *et al*., 2006). Among the Se compounds which may become in contact with cells, selenite is prooxidant because it causes glutathione-mediated reduction to hydrogen selenide and subsequent formation of superoxide radical, which can undergo conversion into other ROS (Chen *et al.*, 2007; Spallholz, 1997; Tarze *et al*., 2007). *Saccharomyces cerevisiae* is an adequate organism to study the toxic properties of Se and the cellular mechanisms which prevent or repair its effects, without the interference due to Se requirement for selenoproteins. In fact, *S. cerevisiae*, and fungi in general, do not contain selenoproteins and therefore, Se is not essential for these organisms (Lu & Holmgren, 2009). High concentrations of Se cause DNA double-strand breaks in exponentially-growing *S. cerevisiae* cells (Letavayová *et al*., 2008) and *RAD9*-dependent cell cycle arrest (Pinson *et al*., 2000). In accordance, yeast mutants defective in the *RAD9*-mediated DNA repair pathway or the *RAD6*/*RAD18*-mediated DNA damage tolerance pathway are hypersensitive to sodium selenite (Seitomer *et al*., 2008), pointing to the importance of DNA damage to explain Se toxicity on yeast cells. Mutant analyses have also demonstrated the importance of the base excision repair pathway in tolerance against selenite (Mániková *et al.,* 2010).

Transcriptome analysis of selenite-treated *S. cerevisiae* cells reveals overlapping between the Se and oxidative stress responses, by the common upregulation of genes for oxidoreductases and for proteasome protein components (Salin *et al*., 2008). This suggests that Se also causes damage on proteins. Yeast cells react to oxidative stress by synthesizing enzymes for ROS detoxification and for repairing macromolecular oxidative damage (Herrero *et*

al., 2008). GRXs are thiol oxidoreductases that regulate the redox state of cysteine sulfhydryl groups (a main target of protein oxidants), by using GSH as reductant (Lillig *et al*., 2008). *S. cerevisiae* contains eight GRXs (Grx1p to Grx8p) which are in different cell compartments. Dithiol GRXs Grx1p and Grx2p (CPYC active site) are mainly cytosolic, but a minor part of Grx2p is located at mitochondria (Luikenhuis *et al.*, 1998; Porras *et al*., 2006). Despite the proposed role of Grx1p and Grx2p as general thiol oxidoreductases, their absence causes only moderate hypersensitivity to superoxide (in the case of Grx1p) and to superoxide and hydroperoxide (in the case of Grx2p) (Eckers *et al.*, 2009; Luikenhuis *et al*., 1998). This phenotype could be explained based on the activity of these GRXs as glutathione peroxidases in *in vitro* assays (Collinson *et al*., 2002). Surprisingly, a *grx2* mutant displays higher survival rates than wild type cells in the presence of cadmium, which indirectly causes oxidative stress through deprivation of GSH (Gomes *et al*., 2008). Grx3p, Grx4p and Grx5p are monothiol GRXs (CGFS active site) and may have specialized functions related to iron homeostasis and iron-sulphur cluster synthesis at mitochondria (Herrero & de la Torre-Ruiz, 2007; Pujol-Carrión *et al*., 2006; Rodríguez-Manzaneque *et al*., 1999). Grx6p and Grx7p are associated to membranes of the early secretory pathway, although their function is unknown (Izquierdo *et al*., 2008; Mesecke *et al*., 2008a; Mesecke *et al*., 2008b). They have a single-cysteine active site, but their amino acid sequences are more similar to dithiol GRXs. Finally, Grx8p is a cytoplasmic dithiol enzyme with a non-standard CPDC active-site and low activity *in vitro* (Eckers *et al*., 2009). Its absence does not cause significant growth phenotypes.

After application of diverse cellular stresses, *S. cerevisiae* cells may undergo apoptosis-like death (Madeo *et al.*, 1999; Madeo *et al*., 2004). Oxidative stress is among the apoptosis inducers in yeast (Perrone *et al*., 2008). Thus, hydrogen peroxide at low concentrations provokes apoptosis in a process dependent on the metacaspase Yca1p and on a functional mitochondrial respiratory chain, while high peroxide concentrations provoke non-apoptotic death (Khan *et al.*, 2005; Madeo *et al*., 1999; Madeo *et al*., 2002). Several metals and metalloids also cause apoptosis in yeast cells, probably related to their role in ROS formation. Thus, copper induces ROS-mediated apoptosis dependent on

functional mitochondria, but not on Yca1p (Liang & Zhou, 2007). Manganese is also an inducer of mitochondria-dependent apoptosis, but contrary to copper, apoptotic death by manganese depends on Yca1p and does not correlate with intracellular ROS accumulation (Liang & Zhou, 2007). Low cadmium concentrations induce Yca1p-dependent apoptosis in *S. cerevisiae*, probably as a consequence of intracellular GSH depletion and redox unbalance (Gomes *et al*., 2008; Nargund *et al*., 2008). Arsenite also causes glutathione depletion and Yca1- and mitochondria-dependent apoptosis in yeast cells (Du *et al*., 2007). These observations corroborate the existence of multiple pathways leading to apoptosis in yeast cells. On the other hand, a number of yeast cell treatments lead to non-apoptotic death (sometimes referred as necrotic death) characterized by loss of plasma membrane integrity and consequent permeability to agents such as methylene blue or propidium iodide (Dudgeon *et al*., 2008; Madeo *et al*., 1999).

Recently, it was reported that a *S. cerevisiae* mutant lacking Grx1p and Grx2p shows increased growth sensitivity to selenite (Lewinska & Bartosz, 2008). This opened the possibility to study the relationship between GRXs and protection against Se toxicity. In this study, we demonstrate that selenite causes both non-apoptotic and apoptotic death, and that Grx1p and Grx2p protect against non-apoptotic death but not against apoptotic death. We also characterize Se-induced apoptosis, and employ the sensitivity phenotype of the *grx1 grx2* mutant to study how other yeast GRXs are able to replace Grx1p and Grx2p functions in relation to protection against Se toxicity.

METHODS

Strains, plasmids and growth conditions. The *S. cerevisiae* strains used in this work are listed in Table 1. Except when indicated, they are derived from wild type strain W303-1A (*MAT***a** *ade2-1 his3-1 leu2-3,112 trp1-1 ura3-1 can1-100*). Knockout strains have the respective open reading frame substituted by the indicated genetic marker, and they were obtained by standard procedures

(Sherman, 2002) or after successive backcrosses of the mutants with the wild type strain.

Plasmids pMM902 and pMM903 contain the respective coding sequences of *GRX7* and *GRX6* from codon 44 fused to an initial methionine codon, under the control of a $tetO_7$ promoter in the *URA3* vector pMM110. This is an integrative vector similar to other doxycycline-regulated expression plasmids described in Garí *et* al. (1997), obtained by moving a *Eco*RI-*Hind*III fragment with the tTA transactivator plus the $tetO_7$ promoter and the *ADH1* terminator from pCM190, into the YIplac211 vector (Gietz & Sugino, 1988). pMM960 derives from pMM902 by introducing a Cys to Ser substitution in the CPYS active site sequence of the *GRX7* open reading frame, using the ExSite method for creating point mutations (Weiner & Costa, 1995). Introduction of the desired mutation was confirmed by DNA sequencing. Integrative plasmid pMM950 contains the *GRX1* open reading frame plus the own promoter and terminator sequences (783 and 357 base pairs respectively), cloned in YIplac211. Plasmid pMM952 derives from pMM98 (Rodríguez-Manzaneque *et al*., 2002) by moving a *Pst*I-*BamH*I region which expresses a cytosolic form of Grx5p, into YIplac211. Constructions were checked by DNA sequencing. Plasmids were chromosomally integrated at the *URA3* locus after linearization by *Eco*RV digestion.

Cells were usually grown at 30ºC in YPD medium [1% (w/v) yeast extract, 2% (w/v) peptone, 2% (w/v) glucose]. Liquid cultures that had been growing exponentially for at least ten generations were employed before sodium selenite (Sigma) addition. This was generally added at 6 mM concentration. Both untreated and treated cultures were always maintained at concentrations lower than $4x10^7$ cells ml^{-1} (equivalent to exponential growth conditions in untreated cultures), to avoid nutrient starvation effects. With this objective, dilutions with prewarmed fresh medium without or with selenite were made when required. For respiratory growth, YPGly medium was employed, with the same composition as YPD except that it contains 3% (w/v) glycerol instead of glucose.

Growth determinations. Total cell number was determined using a Coulter Z2 analyzer, after 2% (w/v) formaldehyde fixation of cell culture samples. Viable cells were quantified by plating adequate dilutions of culture samples on YPD plates, and counting the colony forming units after two days of incubation at 30ºC. Sensitivity to selenite was also determined in plate assays by spotting serial 1:10 dilutions of exponentially cultures onto YPD plates containing sodium selenite, and recording growth after two days of incubation at 30ºC.

Cell death assays. About 2 x 10^6 cells from YPD medium cultures were centrifuged at room temperature, washed with synthetic SC medium (Sherman, 2002) and resuspended in 20 µl of fresh SC medium containing 200 µg methylene blue or propidium iodide ml^{-1}. Stained (dead) and unstained (alive) cells were counted under phase contrast microscopy. At least 200 cells were counted per sample.

TUNEL assays. About 2 x 10^7 cells were harvested, washed with water and fixed with 500 µl of 3.7% (v/v) formaldehyde in PBS during 30 min at room temperature. Cells were then washed with PBS and resuspended in 50 µl of PBS with 300 µg Zymolyase 100T (ICN Biomedicals) ml^{-1}. Incubation was carried out at 30 ºC, and was followed by phase contrast microscopy until spheroplast formation. Cells were then washed by gentle centrifugation, applied to polylysine-coated slide wells and allowed to settle for 15 min at room temperature. Excess liquid was removed, cells were washed with PBS and each well was incubated with 20 µl of permeabilization solution [0.1% (v/v) Triton X-100 in a 0.1% (w/v) sodium citrate solution] during 2 min at 4 ºC. After two washes with PBS, 15 µl of TUNEL Reaction Mixture (In Situ Cell Death Detection kit, Fluorescein; from Roche Applied Science) were applied to each well, for DNA free 3'-OH termini labeling with fluorescein isothiocyanate (FITC)-dUTP. The reaction was done following the kit instructions, with incubation at 37 ºC for one hour. After three rinses with PBS, the preparation was dried for 10 min at room temperature and mounted with 4 µl of Slowfade Gold antifade reagent (Molecular Probes). For scoring the percentage of cells with fluorescent nuclei, at least 200 cells were observed per sample, in an Olympus BZ51

fluorescence microscope with a U-MNBA3 filter for FITC emission. In parallel, positive controls were done which consisted of permeabilized cells treated for 10 min at room temperature with 0.1 μgDNAse I (Sigma) ml^{-1}.

Mutagenicity assays. Culture samples were taken, washed with synthetic SD medium (Sherman, 2002), and resuspended in this medium. Equivalents between 2 x 10^6 and 2 x 10^7 cells were plated onto SD plates added with the required auxotrophic supplements plus canavanine (60 μg ml^{-1}). In parallel, adequate dilutions were plated onto the same medium without canavanine, to determine the concentration of viable cells. Number of growing colonies on the respective plates was counted after 3 days of incubation at 30 ºC, to calculate the fraction of viable cells which were canavanine-resistant.

DAPI staining. Nuclei were stained with DAPI. About 1 x 10^7 cells were harvested, washed with PBS and fixed with 3.7% (v/v) formaldehyde in PBS during 30 min. After three washes with PBS, cells were incubated with DAPI (2 μg ml^{-1}) in PBS in the dark, which was followed by a wash in PBS and fluorescence microscopy analysis.

Western blot analyses. Western blot analyses were done according to Bellí *et al*., 1998. Anti-Grx7p antibodies (Mesecke *et al*., 2008) were employed at a 1:500 dilution.

Protein carbonylation analyses. Analysis of protein carbonylation after derivatization of carbonyl groups with DNPH was carried out as described in Molina *et al*. (2004), except that rabbit anti-DNPH antibodies (Sigma) were employed at 1:2,000 dilution.

ROS determinations. Dihydroethidium is a fluorescent probe for ROS detection which shows some selectivity for superoxide anion (Benov *et al*., 1998). About 10^7 cells were harvested, washed with PBS and resuspended in 1 ml of PBS plus 0.1% glycerol. Fluorescence emission was measured at time 0 and then dihydroethidium (Sigma) was added (5 μg μl^{-1} final concentration).

Fluorescence measurements were made at 5 min intervals during 30 min, using a λ_{ex} of 520 nm and λ_{em} a 590 nm. Relative emission rate was calculated from the slope of the linear regression data plot.

RESULTS

Grx1p and Grx2p have overlapping roles in protecting against selenite toxicity in *S. cerevisiae,* and can be substituted by other GRXs

It has been reported that a *grx1 grx2* mutant of *S. cerevisiae* is hypersensitive to sodium selenite (Lewinska & Bartosz, 2008). We confirmed this observation in the W303 genetic background employed in our experiments, and observed that the single *grx1* or *grx2* mutants display the same sensitivity as wild type cells in plate growth assays (Fig. 1A), which indicates that both GRXs have overlapping functions in protection against selenite toxicity. When the double mutant was transformed with an integrative plasmid (pMM958) that expressed *GRX1* under its own promoter, the phenotype was rescued (Fig. 1A), demonstrating that the hypersensitivity of the mutant to selenite was exclusively caused by the absence of both GRXs. Similar results were obtained with an integrative plasmid expressing *GRX2* at physiological levels (not shown).

Some yeast GRXs may have interchangeable activities provided that compartmental barriers are eliminated (Molina *et al*., 2004). The sensitivity phenotype of the *grx1 grx2* mutant allowed us to determine whether membrane-associated GRXs can carry out the functions of classical dithiol GRXs when the former are targeted to the cytosol. For cytosolic compartmentalization, we used constructions that expressed truncated forms of Grx6p or Grx7p without the transmembrane domain, under the control of the doxycicline-regulated $tetO_7$ promoter. The Grx6p and Grx7p forms that lack the transmembrane domain in fact localize at the cytosol (Izquierdo *et al*., 2008). These cytosolic versions conferred to the double mutant almost the same level of resistance to selenite on YPD plates as wild type cells (Fig. 1B). Although further studies are described here for Grx7p, similar rescuing properties were observed for Grx6p

(data not shown). The protective function of Grx7p against selenite depended on its thiol oxidoreductase activity, since substitution of the cysteine residue of its CPYS active site by a serine abrogated such function (Fig. 1B). The possibility existed that the rescuing ability of Grx7p was caused by non-physiological overexpression of the protein. However, this does not seem to be the case, since western analysis demonstrated that the levels of cytosolic Grx7p are similar to those of the native membrane-associated form of the protein expressed under its own promoter (Fig. 1C). As expected, doxycycline addition drastically reduced Grx7p levels. As demonstrated in a previous study (Izquierdo *et al*., 2008), cytosolic Grx7p run in the gels as a homogeneous form, while the membrane-associated protein exhibited multiple bands due to O-glycosidic modifications (Fig. 1C). We also tested whether a monothiol GRX of the CGFS type, Grx5p, which normally localizes at mitochondria (Rodríguez-Manzaneque *et al*., 2002), is able to substitute for the Grx1p and Grx2p role when artificially localized at the cytosol. However, functional substitution did not occur, since the mitochondrial targeting sequence-less derivative of Grx5p did not rescue the selenite hypersensitivity of the *grx1 grx2* mutant (Fig. 1B). Overall, the observations support the structural and biochemical proximity of Grx6p and Grx7p to dithiol GRXs, and are in accordance with previous results showing that Grx1p and Grx2p do not substitute for the mitochondrial function of Grx5p in the synthesis of iron-sulphur clusters (Molina *et al*., 2004).

Selenite causes non-apoptotic and apoptotic death in yeast cells

To further characterize the effect of Se on yeast cells and the protective role of Grx1p/Grx2p, the growth rate of wild type and *grx1 grx2* mutant cells was quantified in liquid cultures in YPD medium (fermentative growth) in the presence of sodium selenite (Fig. 2A). In order to maintain exponential conditions for treated and non-treated cells during the experiment time course, cultures were successively diluted into fresh medium without or with selenite when required (see Methods). Growth rate of treated wild type cultures during the first 24 hours of treatment was about 25% relative to the exponential growth rate of the respective untreated cultures. This was also the case for mutant cell cultures expressing cytosolic Grx7p. In contrast, during the same period of

293 treatment the double mutant grew in the presence of selenite at a rate that was
294 only 15 % that of untreated cultures. After 24 hours of treatment, growth of the
295 three treated cultures became almost totally arrested, and the relative biomass
296 concentration reached by the selenite-treated *grx1 grx2* cultures was about 15%
297 that of the other two treated cultures (Fig. 2A, inbox). These results confirm that
298 cytosolic Grx7p rescues the double mutant phenotype, and also indicate that
299 independently of the strain, growth only becomes totally arrested after 24 hours
300 in the presence of the toxic agent.
301
302 The above results could be due to a growth rate reduction by selenite or to a
303 death effect in part of the population. To distinguish between both possibilities,
304 we determined the fraction of live cells in cultures along 30 hours of selenite
305 treatment. As above, cultures were rediluted when required with fresh medium
306 containing selenite to avoid growth effects by nutrient depletion. From the
307 beginning of treatment, selenite caused progressive accumulation of dead cells,
308 at a larger extent in the *grx1 grx2* mutant than in wild type cells (Fig. 2B). After
309 30 hours of treatment, only 25% and 12% of the cells remained viable
310 respectively in wild type and *grx1 grx2* cultures. The percentage of viable cells
311 in selenite-treated mutant cultures expressing cytosolic Grx7p increased relative
312 to the mutant, although it did not reach the levels of wild type cultures (Fig. 2C).
313 As a control, expression of *GRX1* at physiological levels in an integrative
314 plasmid (pMM958) in the chromosomal *grx1 grx2* background rescued viability
315 of selenite-treated cultures to the same levels as wild type cells (Fig. 2C).
316
317 We next determined the type of death caused by selenite in *S. cerevisiae*, and
318 how the absence of Grx1p and Grx2p influenced death rate. Different markers
319 can be used in yeast cells to distinguish between non-apoptotic and apoptotic
320 death. In the case of non-apoptotic death, the process is accompanied by an
321 increase of plasma membrane disorganization and permeability to staining
322 agents such as propidium iodide or methylene blue (Dudgeon *et al*., 2008;
323 Zhang *et al*., 2006). In experiments using the latter agent, plasma membrane-
324 compromised cells began appearing at early times of treatment and increased
325 in number progressively (Fig. 3). Up to 18 hours of treatment, the proportion of
326 dead cells in the population was significantly higher in the double mutant than in

wild type cells. The differences were statistically significant, as determined with a Kluskal-Wallis test, and expression of cytosolic Grx7p reduced the amount of methylene blue-permeable dead cells. At later times of treatment (24 hours), the percentage of cells with compromised plasma membrane did not show statistically significant differences among the three cultures (around 40% in all cases). Similar values were obtained with propidium iodide as non-apoptotic death marker (data not shown). This therefore indicates that Grx1p and Grx2p functions make cells less susceptible to the early toxic events induced by selenite which lead to non-apoptotic cell death. In all cases, 70±3% of the plasma membrane-compromised cells had buds, which is a percentage very similar to the entire population. This suggests that non-apoptotic death does not specifically affect to cells at particular cell cycle stages.

We also determined whether selenite-treated *S. cerevisiae* cells displayed apoptotic markers. A marker appearing at initial stages of yeast apoptosis is nuclei degeneration (half-ring shaped) followed by fragmentation (Madeo *et al*., 1999), which can be evidenced by DAPI staining. In fact, some few abnormal nuclei began to appear in wild type cells after 12 hours of selenite treatment, while after 24 hours a significant fraction of the cell population contained fragmented nuclei (Fig. 4A). This pointed to apoptotic death caused by selenite. In order to quantify apoptotic cells in wild type and *grx1 grx2* cells treated with selenite, we used the cleavage of chromosomal DNA producing free 3'-OH termini as an apoptotic marker widely used in yeast cells. These DNA termini can be detected by the TUNEL assay in the form of fluorescent nuclei (Madeo *et al*., 1999; Madeo *et al*., 2002). TUNEL-positive wild type cells appeared at a significant proportion (more than 40% of the population) after 24 hours of treatment (Fig. 4B and C). At this time, no differences were observed in the percentage of budded cells between TUNEL-positive and -negative cells (data not shown). When we quantified cultures of the *grx1 grx2* mutant non-expressing or expressing the cytosolic Grx7p form (Fig. 4C), no significant statistical differences (as determined with a Kluskal-Wallis test) in the proportion of TUNEL-positive cells were observed compared to the wild type strain. This confirms that selenite also causes apoptotic death after long times of exposition, and that Grx1p and Grx2p do not seem to protect against this type of death.

Selenite-mediated non-apoptotic and apoptotic dead cells are independent populations

The possibility existed that membrane-compromised and TUNEL-positive populations overlapped, in other words, that the death markers employed by us did not inform about the existence of two independent death events, at least at advanced treatment times. However, two different experimental evidences support the independence of both types of death in selenite-treated yeast cells, in addition to the above described differential dependence on Grx1p and Grx2p functions. First, we treated wild type cells for 24 h with lower selenite concentrations (3 and 4 mM). In these conditions a significant number of cells still displayed non-apoptotic death markers, while the proportion of TUNEL-positive cells remained almost negligible (Fig. 4D). After the 24 h treatment at 4 mM selenite, almost 14% of the cells were membrane-compromised while less than 2% of the cells displayed an apoptotic marker. Second, we treated wild type cells with 6 mM selenite for 24 h and then we simultaneously stained them with propidium iodide and DAPI, without previous formaldehyde fixation. In these conditions, only about 10% of the cells showing abnormal nuclear morphology were also permeable to propidium iodide. Taken together, these observations support the idea that the apoptosis-like nuclear alterations in selenite-treated cells are not secondary to long-term membrane alterations in dead cells, and that there is only a minor overlapping between non-apoptotic and apoptotic dead cell populations.

Selenite-mediated apoptosis requires Aif1p activity

Yeast Yca1p metacaspase mediates apoptosis induced by hydrogen peroxide (Khan *et al*., 2005; Madeo *et al.*, 2002) or other stimuli (Madeo *et al*., 2004; Mazzoni & Falcone, 2008). However, agents such as copper provoke apoptosis by an Yca1p-independent mechanism (Liang & Zhou, 2007). We therefore studied whether apoptosis induced by selenite depends on Yca1p. A null *yca1* mutant showed a slightly reduced percentage of TUNEL-positive cells compared with the wild type strain upon treatment with the agent (Fig. 5A), and

its growth was not significantly affected in plate assays in the presence of selenite (data not shown). This indicates that Yca1p has only a modest role in mediating apoptotic death by selenite.

Mitochondrial functions are required for apoptosis induction by different agents (Pereira *et al*., 2008). Thus, mutational disruption of the *S. cerevisiae* mitochondrial electron transport chain reduces apoptosis caused by copper and manganese (Liang & Zhou, 2007), amiodarone (Pozniakovsky *et al*., 2005), acetic acid (Ludovico *et al*., 2002), hyperosmotic stress (Silva *et al*., 2005) or chronological aging (Li *et al*., 2006). We tested how the absence of Ndi1p (mitochondrial inner membrane-associated NADH dehydrogenase) or Cox12p (part of complex IV in the electron transport chain) affected selenite-induced apoptosis. The *ndi1* mutant displayed a moderate reduction of TUNEL positive cells, while the percentage of TUNEL positive cells in the *cox12* mutant was similar to the wild type strain (Fig. 5A). No differences in growth were observed in both mutants compared to wild type cells in a plate growth assay in the presence of selenite (data not shown). Therefore, disruption of the mitochondrial electron transport chain has moderate or no effect on induction of apoptosis by selenite.

Yeast Aif1p protein is the homologue of AIF, a mammalian mitochondrial flavoprotein which upon apoptotic stimuli translocates into the nucleus, where it plays a role in caspase-independent induction of apoptosis (Susin *et al*., 1999). AIF has oxidoreductase activity, although conflicting data exist whether this and the apoptosis-induction activity are functionally independent or not (Churbanova *et al*., 2008; Miramar *et al*., 2001). In *S. cerevisiae*, Aif1p mediates apoptosis induced by oxidative stress, acetic acid or chronological aging (Wissing *et al*., 2004), and it is also important for survival upon manganese treatment (Liang & Zhou, 2007). On the contrary, it does not participate in hyperosmotic stress-induced apoptosis (Silva *et al*., 2005). Upon selenite treatment, the percentage of TUNEL-positive cells was near zero in a null *aif1* mutant (Fig. 5A). In accordance with this, growth inhibition by selenite was slightly lower in the mutant compared to the wild type in a plate growth assay (data not shown). In addition, we compared the percentage of viable cells in liquid cultures of wild

type and *aif1* strains (Fig. 5B). At initial times after selenite addition no differences were observed between both strains, while at extended treatment times (24 and 30 hours) cell viability was 2.5 to 3-fold higher in the mutant. Considering the kinetics in Fig. 2B, we can conclude that parallelism between both strains only occurs at the non-apoptotic death phase, while during apoptotic death the *aif1* cells do not become further affected by selenite. Summarizing, Aif1p seems to be a mediator of apoptosis induced by selenite in yeast cells.

To further investigate the participation of mitochondrial functions in selenite-mediated apoptosis, we analyzed the effect of this agent on yeast cells growing in respiratory conditions (YPGly medium). Much lower concentrations were required than in glucose-based medium to reach similar growth inhibition levels (Fig. 5C). However, at concentrations lower than 0.2 mM, growth inhibition by selenite was exclusively due to growth rate reduction, since practically all cells in the population remained viable (as determined by plate growth assays and comparison with total cell determinations, data not shown). Also in contrast with the effects in YPD medium, selenite did not cause the appearance of membrane-permeable dead cells at concentrations that provoked apoptotic death (Fig. 5C). Only at selenite concentrations of 1 mM or higher methylene-blue stained cells were observed. That is, in respiratory conditions apoptotic death by selenite precedes other death effects. Mutants lacking Yca1p or Ndi1p displayed levels of TUNEL-positive cells about 50% those of wild type cells (data not shown), which indicates that in YPGly medium selenite-induced apoptosis is also only partially dependent on Yca1p or Ndi1p. We could not determine the role of Aif1p in these conditions, since the *aif1* mutant had an extremely defective growth in YPGly medium.

Selenite provokes an increase of protein carbonylation

Protein carbonylation is a consequence of oxidative stress on yeast cells (Cabiscol *et al*., 2000), and can be used as a marker of protein damage by oxidants. We performed carbonylation assays with total cell extracts from wild

type and *grx1 grx2* cultures after different times of selenite treatment in YPD medium (Fig. 6A). No differences were observed between the two strains in non-treated cultures and at initial times of treatment. However, after 18 and 24 hours selenite caused more extensive protein carbonylation in the double mutant than in wild type cells. Expression of cytosolic Grx7p in the mutant abolished such differences (Fig. 6A). Loading controls (Coommassie blue staining of gels) indicated that the approximately the same protein amount was loaded in all lanes. We conclude that accumulation of carbonyl modifications in proteins could be a consequence of the ROS generated by selenite.

Diverse studies have shown that apoptotic cells can be a source of ROS, and therefore of oxidative damage (Perrone *et al*., 2008). Consequently, we determined protein carbonylation in *aif1* cells after 24 hours of selenite treatment, compared to wild type cells. Both wild type and *aif1* cells displayed considerable protein carbonylation in gels upon treatment, although the levels were lower in the mutant even at the 7 mM selenite concentration employed in this experiment (Fig. 6B). Therefore, apoptosis inhibition reduces protein carbonyl levels, suggesting that a fraction of the protein carbonyl groups which accumulate after prolonged treatment with selenite results from ROS generated by apoptotic cells.

To confirm intracellular ROS accumulation at late times of selenite treatment, we employed dihydroethidium as a fluorescent probe for ROS which has some selectivity for superoxide anions (Benov *et al*., 1998). In wild type cells, fluorescence emission increased 2 to 3-fold (relative to time 0) only after 24 hours in the continuous presence of selenite (Fig. 6C), that is, in parallel to the accumulation of apoptotic cells. At shorter treatment times, fluorescence emission due to ROS accumulation remained at levels similar to untreated cells. Such fluorescence emission at advanced treatment times was significantly lower in the *aif1* mutant (Fig. 6C). Remarkably, untreated exponentially-growing *aif1* cells contain abnormally high intracellular levels of ROS, which may be related to disruption of the mitochondrial function of Aif1p in the mutant. Overall, these results support that selenite-induced apoptotic cells are a source of ROS.

Selenite mutagenicity is higher in the absence of Grx1 and Grx2

We also determined Se-mediated genotoxicity in the *grx1 grx2* mutant and in wild type cells, based on the appearance of canavanine-resistant (can^R) mutants among the population of viable cells. Since the genetic background (W303) employed in the previous experiments was already can^R, the following experiments were done in a different background of canavanine-sensitive wild type cells and its corresponding *grx1 grx2* derivative. The effect of selenite on the cell viability in this new background was similar to that shown in Fig. 2B for the respective W303 background strains (data not shown). As expected from Pinson *et al.* (2000), the proportion of wild type viable cells which became can^R increased with time of selenite treatment, confirming the mutagenicity by selenite in our experimental conditions (Fig. 7A). However, the proportion of can^R mutants among viable cells was considerably higher in the *grx1 grx2* strain, especially at the initial periods of treatment. This confirmed that Grx1p and Grx2p also protect against selenite-caused genotoxicity. In a double mutant expressing the cytosolic version of Grx7p, the frequency of can^R mutants was similar to wild type cells (Fig. 7B), confirming that expression of Grx7p at the cytosol also suppressed the increased genotoxicity of selenite in the *grx1 grx2* mutant.

DISCUSSION

In contrast to higher organisms, Se is not an essential oligoelement for yeast cell growth. Instead, high concentrations of Se cause genotoxicity in *S. cerevisiae*. The more toxic form of Se is selenide, which can be formed either outside or inside the cell from other Se forms, such as selenite (Tarze *et al*., 2007). Oxidation of selenide may generate superoxide which then can be converted into other ROS to oxidize cellular components (Chen *et al*., 2007; Spallholz, 1997). Analysis of the sensitivity to Se of a large collection of *S. cerevisiae* null mutants indicated that the majority of the hypersensitive mutants

530 are affected in DNA repair functions (Seitomer *et al*., 2008), supporting the
531 importance of DNA damage in Se toxicity.
532
533 In this work, we show that under fermentative growth selenite causes non-
534 apoptotic death at initial times of treatment, while longer treatment induces
535 apoptosis. This contrasts with peroxide-induced apoptosis in yeast (Madeo *et*
536 *al*., 1999). In the latter case, low oxidant doses cause apoptosis, while a more
537 intense stress produces so-called necrotic death. In the case of selenite,
538 lowering the concentration does not increase the apoptosis rate. However, the
539 experimental conditions were different for both types of experiments: while a
540 single peroxide dose was given (Madeo *et al.*, 1999), in the case of selenite this
541 was maintained in the presence of the cells for longer times by repeated dilution
542 with prewarmed medium containing the agent. At initial treatment times with
543 selenite (up to 18 hours) when appearance of apoptotic markers is negligible,
544 the observed viability decrease can be attributed to non-apoptotic death. At
545 these initial times, the percentage of dead cells as determined by plate assays
546 is higher than the percentage of methylene blue-permeable cells, suggesting
547 that some of the dead cells may initially maintain the plasma membrane
548 integrity. In any case, the population fraction of membrane-compromised cells
549 increases steadily along treatment. In contrast to the effects on cells growing
550 under fermentative metabolism, during respiratory growth low doses of selenite
551 preferentially provoke apoptotic death, and non-apoptotic necrotic-like death
552 only occurs at high doses of the agent, that is, a situation reminiscent of the
553 peroxide death effects.
554
555 Grx1p and Grx2p have an overlapping role in protection against selenite-
556 induced non-apoptotic death. A protective role against selenate (another toxic
557 form of Se) has been reported for the Grx1p homologue in a cyanobacterium
558 (Marteyn *et al*., 2009). We can only speculate about the function of both yeast
559 GRXs in relation to Se toxicity. Considering the redox regulatory role of GRXs
560 on protein cysteine residues, one obvious possibility is that Grx1p and Grx2p
561 would target proteins important for protection against selenite damage. Given
562 the genotoxicity of selenite at the concentrations used in this study, some of the
563 proteins involved in DNA repair and damage tolerance would be candidates for

being regulated by Grx1p/Grx2p activity. Alternatively, Grx1p and Grx2p could have a more unspecific role, perhaps based on their peroxidase activity (Collinson *et al*., 2002). In fact, high concentrations of selenite generate ROS in many cell types (Latavayová *et al*., 2006) and here we have shown that it causes time and concentration-dependent protein carbonylation and ROS accumulation being indicative of intracellular oxidative stress. That selenite-induced redox disturbance is important for yeast cell growth is supported by the fact that antioxidants such as N-acetylcysteine rescue the growth defects (Lewinska & Bartosz, 2008).

The importance of GSH-mediated protection against Se is confirmed by observations from two global analyses in *S. cerevisiae*: (i) the overrepresentation of mutants in GSH-mediated pathways among those mutants displaying selenite hypersensitivity (Seitomer *et al*., 2008); and (ii) the transcriptional induction of genes involved in these same pathways upon selenite treatment (Salin *et al*., 2008). In this context, decreasing the ratio between GSH and oxidized glutathione after selenite-induced oxidative stress would influence cell viability. In addition, the mentioned transcriptomic study suggests that selenite may also influence intracellular iron homeostasis by interfering with mitochondrial iron-sulphur cluster synthesis (Salin *et al*., 2008). The results of the present study demonstrating the importance of GSH-dependent Grx1p and Grx2p activity for protection against non-apoptotic death emphasize the role of GSH in defence against Se toxicity.

When targeted to the cytosol, Grx6p and Grx7p rescue the accumulation of membrane-compromised cells in the *grx1 grx2* mutant, as well as the accumulation of carbonylated proteins and the mutagenicity rate, to wild type levels. This proves that their function as GRXs can protect against Se toxicity. Thus, compartmental barriers do not necessarily correlate with functional barriers, as is also the case with other GRXs (Molina *et al*., 2004). Our observations also show that protection against selenite toxicity by GRXs requires a single active site cysteine and therefore, a monothiol mechanism of action. Remarkably, deglutathionylation of mixed disulphides between GSH and cysteine sulfhydryl groups of proteins only require the most N-terminal cysteine

of the GRX active site (Bushweller *et al*., 1992). This is also the case of Grx1p in the defence against selenite action. Therefore, the possible functions of Grx1p and Grx2p could be related to redox repair of glutathionylated cysteine residues produced under selenite stress.

S. cerevisiae cells which survive to initial non-apoptotic death in YPD medium may suffer apoptotic death at advanced times of selenite treatment. Grx1p and Grx2p do not play a protective role against this type of death, which is also not affected by cytosolic expression of Grx7p. Therefore, hyperaccumulation of oxidatively-damaged proteins can not be the signal triggering selenite-induced apoptosis. Several metals and metalloids are inductors of apoptosis in yeast cells, through mechanisms which may involve diverse intermediates (Gomes *et al*., 2008; Liang & Zhou, 2007). In the case of selenite, neither Yca1p metacaspase nor a functional mitochondrial electron transport chain plays a major role in apoptosis induction, a situation which extends to apoptotic death during respiratory growth. In mammalian cells, AIF and AMID (AIF-homologous mitochondrion-associated inducer of death) are mediators of caspase-independent apoptosis (Cande *et al*., 2002; Wu *et al*., 2002). Yeast Ndi1p is homologous to mammalian AMID (Li *et al*., 2006). In the absence of Ndi1p there is only a moderate reduction of apoptosis in selenite-treated cells. On the other hand, Aif1p seems to be central in apoptosis induction by selenite in *S. cerevisiae*. This is similar to apoptosis induction by the antimicrobial peptide dermaseptin S3 in yeast, which also depends on Aif1p but not on Yca1p (Morton *et al.*, 2007). The *in vivo* role of mammalian AIF is a matter of debate. In parallel to (or related with) its apoptosis-promoting function, AIF is important for mitochondrial oxidative phosphorylation (Modjtahdi *et* al., 2006; Vahsen *et* al., 2004). In accordance with this, inhibiting AIF expression causes intracellular ROS accumulation in human cell lines (Apostolova *et al*., 2006). We have also observed ROS hyperaccumulation in the *S. cerevisiae aif1* mutant during exponential growth, which supports a mitochondrial function for yeast Aif1p related to electron transport. In contrast, the *aif1* mutant displays reduced accumulation of carbonylated proteins and of ROS at advanced times of selenite treatment in YPD medium compared to wild type cells, supporting that the apoptotic cells are a source of the oxidative stress generated in that

situation. Apoptotic *S. cerevisiae* cells resulting from a hyperosmotic stress are also a source of ROS (Silva *et al*., 2005).

Summarizing, selenite causes cell death through several mechanisms, including apoptosis, and GRX activity is important to protect cells against non-apoptotic death at initial periods, pointing to the importance of redox control of proteins to overcome Se toxicity. Characterization of the specific protein targets will provide information about the GRXs function in this type of stress.

ACKNOWLEDGEMENTS

We thank Joaquim Ros for critical reading of the manuscript, María Pérez-Sampietro for helping in some experiments, Johannes M. Herrmann for the gift of antibodies, and Mireia Aresté for technical assistance. This work was supported by grants BFU2004-03167 and CSD2007-0020 (Ministerio de Ciencia e Innovación) to E.H. A.I. is the recipient of a grant from Ministerio de Ciencia e Innovación, Spain.

REFERENCES

Apostolova, N., Cervera, A.M., Victor, V.M., Cadenas, S., Sanjuán-Pla, A., Alvarez-Barrientos, A., Espulgues, J.V. & McCreath, K.J. (2006). Loss of apoptosis-inducing factor leads to an increase in reactive oxygen species, and an impairment of respiration that can be reversed by antioxidants. *Cell Death Differ* **13,** 354-357.

Bellí, G., Garí, E., Piedrafita, L., Aldea, M. & Herrero, E. (1998). An activator/repressor dual system allows tight tetracycline-regulated gene expression in budding yeast. *Nucleic Acids Res* **26,** 942-947.

Benov, L., Sztejnberg, L., & Fridovich, I. (1998). Critical evaluation of the use of hydroethidine as a measure of superoxide anion. *Free Rad Biol Med* **25,** 826-831.

Bushweller, J.H., Aslund, F., Wuthrich, K. & Holmgren, A. (1992). Structural and functional characterization of the mutant *Escherichia coli* glutaredoxin (C14-S) and its mixed disulfide with glutathione. *Biochemistry* **31,** 9288-9293.

Cabiscol, E., Piulats, E., Echave, P., Herrero, E. & Ros, J. (2000). Oxidative stress promotes specific protein damage in *Saccharomyces cerevisiae*. *J Biol Chem* **275,** 27393-27398.

Cande, C., Cecconi, F., Dessen, P. & Kroemer, G. (2002). Apoptosis-inducing factor (AIF): key to the conserved caspase-independent pathways of cell death. *J Cell Sci* **115,** 4727-4734.

Chen, J.J., Boylan, L.M., Wu, C.K. & Spallholz, J.E. (2007). Oxidation of glutathione and superoxide generation by inorganic and organic selenium compounds. *Biofactors* **31,** 55-66.

Churbanova, I.Y. & Sevrioukova I.F. (2008). Redox-dependent changes in molecular properties of mitochondrial apoptosis-inducing factor. *J Biol Chem* **283,** 5622-5631.

Collinson, E.J., Wheeler, G.L., Garrido, E.O., Avery, A.M., Avery, S.V. & Grant, C.M. (2002). The yeast glutaredoxins are active as glutathione peroxidases. *J Biol Chem* **277,** 16712-16717.

Du, L., Yu, Y., Chen, J., Liu, Y., Xia, Y., Chen, Q. & Liu, X. (2007). Arsenic induces caspase- and mitochondria-mediated apopotosis in *Saccharomyces cerevisiae*. *FEMS Yeast Res* **7,** 860-865.

Dudgeon, D.D., Zhang, N., Ositelu, O.O., Kim, H. & Cunningham, K.W. (2008). Nonapoptotic death of *Saccharomyces cerevisiae* cells that is stimulated by Hsp90 and inhibited by calcineurin and Cmk2 in response to endoplasmic reticulum stresses. *Eukaryot Cell* **7,** 2037-2051.

Eckers, E., Bien, M., Stroobant, V., Herrmann, J.M. & Deponte, M. (2009). Biochemical characterization of dithiol glutaredoxin 8 from *Saccharomyces cerevisiae*: the catalytic redox mechanism redux. *Biochemistry* **48,** 1410-1423.

Garcerá, A., Barreto, L., Piedrafita, L., Tamarit, J. & Herrero, E. (2006). *Saccharomyces cerevisiae* cells have three omega-class glutathione transferases acting as 1-Cys thiol transferases. *Biochem J* **398,** 187-196.

Garí, E., Piedrafita, L., Aldea, M. & Herrero, E. (1997). A set vectors with a tetracycline-regulatable promoter system for modulated gene expression in *Saccharomyces cerevisiae. Yeast* **13,** 837-848.

Gietz, R.D. & Sugino, A. (1988). New yeast-*Escherichia coli* shuttle vectors constructed with in vitro mutagenized yeast genes lacking six-base pair restriction sites. *Gene* **74,** 3065-3073.

Gomes, D.S., Pereira, M.D., Panek, A.D., Andrade, L.R. & Eleutherio, E.C.A. (2008). Apoptosis as a mechanism for removal of mutated cells of *Saccharomyces cerevisiae*: the role of Grx2 under cadmium exposure. *Biochim Biophys Acta* **1780,** 160-166.

Hatfield, D.L., Berry, M.J. & Gladyshev, V.N. (2006). Selenium: its molecular biology and role in human health, 2nd. ed. New York, NY: Springer-Verlag.

Herrero, E. & de la Torre-Ruiz, M.A. (2007). Monothiol glutaredoxins. a common domain for multiple functions. *Cell Mol Life Sci* **64,**1518-1530.

Herrero, E., Ros, J., Bellí, G. & Cabiscol, E. (2008). Redox control and oxidative stress in yeast cells. *Biochim Biophys Acta* **1780,** 1217-1235.

Izquierdo, A., Casas, C., Mühlenhoff, U., Lillig, C.H. & Herrero, E. (2008). Yeast Grx6 and Grx7 are monothiol glutaredoxins associated with the early secretory pathway. *Eukaryot Cell* **7,** 1415-1426.

Khan, M.A.S., Chock, P.B. & Stadtman, E.R. (2005). Knockout of caspase-like gene, *YCA1*, abrogates apoptosis and elevates oxidized proteins in *Saccharomyces cerevisiae*. *Proc Natl Acad Sci USA* **102,** 17326-17331.

Letavayová, L., Vlasáková, D., Spallholz, J.E., Brozmanová, J. & Chovanec, M. (2008). Toxicity and mutagenicity of selenium compounds in *Saccharomyces cerevisiae*. *Mutat Res* **638,** 1-10.

Letavayová, L., Vlckova, V. & Brozmanová, J. (2006). Selenium: from cancer prevention to DNA damage. *Toxicology* **227,** 1-14.

Lewinska, A. & Bartosz, G. (2008). A role of yeast glutaredoxin genes in selenite-mediated oxidative stress. *Fungal Genet Biol* **45,** 1182-1187.

Li, W., Sun, L., Liang, Q., Wang, J., Mo, W. & Zhou, B. (2006). Yeast AMID homologue Ndi1p displays respiration-restricted apoptotic activity and is involved in chronological aging. *Mol Biol Cell* **17,** 1802-1811.

Liang, Q. & Zhou, B. (2007). Copper and manganese induce yeast apoptosis via different pathways. *Mol Biol Cell* **18,** 4741-4749.

Lillig, C.H., Berndt, C. & Holmgren, A. (2008). Glutaredoxin systems. *Biochim Biophys Acta* **1780,** 1304-1317.

Lu, J. & Holmgren, A. (2009). Selenoproteins. *J Biol Chem* **284,** 723-727.

Ludovico, P., Rodrigues, F., Almeida, A., Silva, M.T., Barrientos, A. & Corte-Real, M. (2002). Cytochrome *c* release and mitochondria involvement in programmed cell death induced by acetic acid in *Saccharomyces cerevisiae. Mol Biol Cell* **13,** 2598-2606.

Luikenhuis, S., Perrone, G., Dawes, I.W. & Grant, C.M. (1998). The yeast *Saccharomyces cerevisiae* contains two glutaredoxin genes that are required for protection against reactive oxygen species. *Mol Biol Cell* **9,** 1081-1091.

Madeo, F., Fröhlich, E., Ligr, M., Grey, M., Sigrist, S.J., Wolf, D.H. & Fröhlich, K.U. (1999). Oxygen stress: a regulator of apoptosis in yeast. *J Cell Biol* **145,** 757-767.

Madeo, F., Herker, E., Maldener, C., Wissing, S., Lachelt, S., Herlan, M., Fehr, M., Lauber, K., Sigrist, S.J., Wesselborg, S. & Fröhlich, K.U. (2002). A caspase-related protease regulates apoptosis in yeast. *Mol Cell* **9,** 911-917.

Madeo, F., Herker, E., Wissing, S., Jungwirth, H., Eisenberg, T. & Fröhlich, K.U. (2004). Apoptosis in yeast. *Curr Opin Microbiol* **7,** 655-660.

Mániková, D., Vlasáková, D., Loduhová, J., Letavayová, L., Vigasová, D., Krascsenitsová, E., Vlcková, V., Brozmanová, J. & Chovanec, M. (2010). Investigations on the role of base excision repair and non-homologous end-joining pathways in sodium selenite-induced toxicity and mutagenicity in *Saccharomyces cerevisiae*. *Mutagenesis* **25,** 155-162.

Marteyn, B., Domain, F., Legrain, P., Chauvat, F. & Cassier-Chauvat, C. (2009). The thioredoxin reductase-glutaredoxins-ferroredoxin crossroad pathway for selenate tolerance in *Synechocystis* PCC6803. *Mol Microbiol* **71,** 520-532.

Mazzoni, C. & Falcone, C. (2008). Caspase-dependent apoptosis in yeast. *Biochim Biophys Acta* **1783,** 1320-1327.

Mesecke, N., Mittler, S., Eckers, E., Herrmann, J.M. & Deponte, M. (2008a). Two novel monothiol glutaredoxins from *Saccharomyces cerevisiae* provide further insight into iron-sulfur cluster binding, oligomerization, and enzymatic activity of glutaredoxins. *Biochemistry* **47,** 1452-1463.

Mesecke, N., Spang, A., Deponte, M. & Herrmann, J.M. (2008b). A novel group of glutaredoxins in the cis-Golgi critical for oxidative stress resistance. *Mol Biol Cell* **19,** 2673-2680.

Miramar, M.D., Costantini, P., Ravagnan, L., Saraiva, L.M., Haouzi, D., Brothers, G., Penninger, J.M., Peleato, M.L., Kroemer, G. & Susin, S.A. (2001). NADH oxidase activity of mitochondrial apoptosis-inducing factor. *J Biol Chem* **276,** 16391-16398.

Modjtahdi, N., Giordanetto, F., Madeo, F. & Kroemer, G. (2006). Apoptosis-inducing factor: vital and lethal. *Trends Cell Biol* **16,** 264-272.

Molina, M.M., Bellí, G., de la Torre, M.A., Rodríguez-Manzaneque, M.T. & Herrero, E. (2004). Nuclear monothiol glutaredoxins of *Saccharomyces cerevisiae* can function as mitochondrial glutaredoxins. *J Biol Chem* **279,** 51923-51930.

Morton, C.O., Costa dos Santos, S. & Coote, P. (2007). An amphibian-derived, cationic, α-helical antimicrobial peptide kills yeast by caspase-independent but AIF-dependent programmed cell death. *Mol. Microbiol.* **65,** 494-507.

Nargund, A.M., Avery, S.V. & Houghton, J.E. (2008). Cadmium induces a heterogeneous and caspase-dependent response in *Saccharomyces cerevisiae*. *Apoptosis* **13,** 811-821.

Pereira, C., Silva, R.D., Saraiva, L., Johansson, B., Sousa, M.J. & Corte-Real, M. (2008). Mitochondria-dependent apoptosis in yeast. *Biochim Biophys Acta* **1783,** 1286-1302.

Perrone, G.G., Tan, S.X. & Dawes, I.W. (2008). Reactive oxygen species and yeast apoptosis. *Biochim Biophys Acta* **1783,** 1354-1368.

Pinson, B., Sagot, I. & Daignan-Fornier, B. (2000). Identification of genes affecting selenite toxicity and resistance in *Saccharomyces cerevisiae*. *Mol Microbiol* **36,** 679-687.

Porras, P., Padilla, C.A., Krayl, M., Voos, W. & Bárcena, J.A. (2006). One single in-frame AUG codon is responsible for a diversity of subcellular localizations of glutaredoxin 2 in *Saccharomyces cerevisiae*. *J Biol Chem* **281,** 16551-16562.

Pozniakovsky, A.I., Knorre, D.A., Markova, O.V., Hyman, A.A., Skulachev, V.P. & Severin, F.F. (2005). Role of mitochondria in the pheromone- and amiodarone-induced programmed death of yeast. *J Cell Biol* **168,** 257-269.

Pujol-Carrión, N., Bellí, G., Herrero, E., Nogués, A. & de la Torre-Ruiz, M.A. (2006). Glutaredoxins Grx3 and Grx4 regulate the nuclear localization of Aft1 and the oxidative stress response in *Saccharomyces cerevisiae*. *J Cell Sci* **119,** 4554-4564.

Rodríguez-Manzaneque, M.T., Ros, J., Cabiscol, E., Sorribas, A. & Herrero, E. (1999). Grx5 glutaredoxin plays a central role in protection against protein oxidative damage in *Saccharomyces cerevisiae*. *Mol Cell Biol* **19,** 8180-8190.

Rodríguez-Manzaneque, M.T., Tamarit, J., Bellí, G., Ros, J. & Herrero, E. (2002). Grx5 is a mitochondrial glutaredoxin required for the activity of iron/sulfur enzymes. *Mol Biol Cell* **13,** 1109-1121.

Salin, H., Fardeau, V., Piccini, E., Lelandais, G., Tanty, V., Lemoine, S., Jacq, C. & Devaux, F. (2008). Structure and properties of transcriptional networks driving selenite stress response in yeasts. *BMC Genomics* **9,** 333.

Seitomer, E., Balar, B., He, D., Copeland, P.R. & Kinzy, T.G. (2008). Analysis of *Saccharomyces cerevisiae* null allele strains identifies a larger role for DNA damage versus oxidative stress pathways in growth inhibition by selenium. *Mol Nutr Food Res* **52,** 1305-1315.

Sherman, F. (2002). Getting started with yeast. *Methods Enzymol* **350,** 3-41.

Silva, R.D., Sotoca, R., Johansson, B., Ludovico, P., Sansonetty, F., Silva, M.T., Peinado, J.M. & Corte-Real, M. (2005). Hyperosmotic stress induces metacaspase- and mitochondria-dependent apoptosis in *Saccharomyces cerevisiae*. *Mol Microbiol* **58,** 824-834.

Spallholz, J.E. (1997). Free radical generation by selenium compounds and their prooxidant toxicity. *Biomed Environ Sci* **10,** 260-270.

Susin, S.A., Lorenzo, H.K., Zamzami, N., Marzo, I., Snow, B.E., Brothers, G.M., Aebersold, R., Siderovski, D.P., Penninger, J.M. & Kroemer, G. (1999). Molecular characterization of mitochondrial apoptosis-inducing factor. *Nature* **397,** 441-446.

Tarze, A., Dauplais, M., Grigoras, I., Lazard, M., Ha-Duong, N.T., Barbier, F., Blanquet, S. & Plateau, P. (2007). Extracellular production of hydrogen selenide accounts for thiol-assisted toxicity of selenite against *Saccharomyces cerevisiae*. *J Biol Chem* **282,** 8759-8767.

Vahsen, N., Candé, C., Brière, J.J., Bénit, P., Joza, N., Larochette, N., Mastroberardino, P.G., Pequignot, M.O., Casares, N., Lazar, V., Feraud, O., Debili, N., Wissing, S., Engelhardt, S., Madeo, F., Piacentini, M., Penninger, J.M., Schägger, H., Rustin, P. & Kroemer, G. (2004). AIF defficiency compromises oxidative phosphorylation. *EMBO J* **23,** 4679-4689.

Wach, A., Brachat, A., Pöhlmann, R. & Philippsen, P. (1994). New heterologous modules for classical or PCR-based gene disruptions in *Saccharomyces cerevisiae*. *Yeast* **13,** 1793-1808.

Weiner, M.P. & Costa, G.L. (1995). Rapid PCR site-directed mutagenesis. In *PCR primer: a Laboratory Manual*, pp. 613-621. Edited by C.W. Dieffenbach & G.S. Dveksler. Cold Spring Harbor, NY: Cold Spring Harbor Laboratory Press.

Wissing, S., Ludovico, P., Herker, E., Büttner, S., Engelhardt, S.M., Decker, T., Link, A., Proksch, A., Rodrigues, F., Corte-Real, M., Fröhlich, K.U., Manns, J., Candé, C., Sigrist, S.J., Kroemer, G. & Madeo, F. (2004). An AIF orthologue regulates apoptosis in yeast. *J Cell Biol* **166,** 969-974.

Wu, M., Xu, L.G., Li, X., Zhai, Z. & Shu, H.B. (2002). AMID, an apoptosis-inducing factor-homologous mitochondrion-associated protein, induces caspase-independent apoptosis. *J Biol Chem* **277,** 25617-25623.

Zhang, N.M., Dudgeon, D.D., Paliwal, S., Levchenko, A., Grote, E. & Cunningham, K.W. (2006). Multiple signaling pathways regulate yeast cell death during the response to mating pheromones. *Mol Biol Cell* **17,** 3409-3422.

TABLE 1. Strains used in this study

Strain	Genotype	Comments
W303-1A	*MAT***a** *ura3-1 ade2-1 leu2-3,112 trp1-1 his3-11,15 can1-1*	Wild type
MML736	W303-1A *grx2::LEU2*	Garcerá *et al.* (2006)
MML751	W303-1A *grx1::kanMX4*	Garcerá *et al.* (2006)
MML752	W303-1A *grx1::kanMX4 grx2::LEU2*	Garcerá *et al.* (2006)
MML1051	MML752 [pMM902(*tetO*$_7$*-GRX7**)]*::URA3*[a]	Integration of pMM902 in MML752
MML1052	MML752 [pMM903(*tetO*$_7$*-GRX6**)]*::URA3*[b]	Integration of pMM903 in MML752
MML1133	W303-1A *yca1::kanMX4*	From the BY4741 background
MML1139	MML752 [pMM952(*GRX5**)]*::URA3*[c]	Integration of pMM952 in MML752
MML1152	MML752 [pMM958(*GRX1*)]*::URA3*	Integration of pMM958 in MML752
MML1157	MML752 [pMM960(*tetO*$_7$*-GRX7*C108S*)]*::URA3*	Integration of pMM960 in MML752
MML1165	W303-1A *ndi1::kanMX4*	From the BY4741 background
MML1166	W303-1A *aif1::kanMX4*	From the BY4741 background
MML1167	W303-1A *cox12::kanMX4*	From the BY4741 background
CML235	*MAT***a** *ura3-52 leu2Δ1 his3Δ200*	Wild type, Rodríguez-Manzaneque *et al.* (1999)
MML1178	CML235 *grx1::kanMX4 grx2::LEU2*	This work
MML1183	MML1178 [pMM902(*tetO*$_7$*-GRX7**)]*::URA3*[a]	Integration of pMM902 in MML1178

[a] *GRX7**: *GRX7* open reading frame without codon 2 to 39
[b] *GRX6**: *GRX6* open reading frame without codon 2 to 39
[c] *GRX5**: *GRX5* open reading frame without codon 2 to 23 (Rodríguez-Manzaneque *et al.*, 2002)

FIGURE LEGENDS

Fig. 1. Effect of 6 mM sodium selenite on *S. cerevisiae* strains in plate growth assays. (A) The following strains were tested for growth in YPD plates without (control) or with selenite (2 days at 30ºC): W303-1A (wild type), MML751 (*Δgrx1*), MML736 (*Δgrx2*), MML752 (*Δgrx1/2*), MML1152 (*Δgrx1/2 GRX1*). (B) The following strains were tested for growth: W303-1A (wild type), MML752 (*Δgrx1/2*), MML1052 (*Δgrx1/2 GRX6**), MML1051 (*Δgrx1/2 GRX7**), MML1139 (*Δgrx1/2 GRX5**), MML1157 (*Δgrx1/2 GRX7*C108S*). (C) Western blot analysis (30 μg of total cell protein per lane) of MML1051 cells expressing both the native Grx7p protein (band a) and the truncated form of Grx7p (band b). The latter form was expressed from the chromosomally-integrated plasmid pMM902, under the control of the $tetO_7$ promoter. In order to modulate expression from the $tetO_7$ promoter, exponential cell cultures in YPD medium at 30ºC were employed with the indicated concentrations of doxycycline.

Fig. 2. Effect of 6 mM sodium selenite on growth of wild type (W303-1A), mutant *Δgrx1/2* cells (strain MML752) and mutant cells expressing a truncated form of Grx7p as indicated in the text (*Δgrx1/2 GRX7*,* strain MML1051). (A) Evolution of total cell number per ml (N) in cultures growing in YPD medium at 30ºC without (filled symbols, continuous lines) or with sodium selenite added at time 0 (empty symbols, dashed lines). N value at time 0 was 10^6 cells ml^{-1}, and cultures were diluted with fresh medium (without or with selenite) when they reached a concentration of 3-4x10^7 cells ml^{-1}. The corresponding dilution factors were considered for plotting N values. Inbox: data of treated cultures plotted in decimal scale. Plots correspond to a representative experiment made in parallel with the three strains. (B) Percentage of viable cells in cultures of wild type or mutant *Δgrx1/2* cells at different times in the presence of sodium selenite. Total cell number and colony forming units (viable cells) ml^{-1} were measured in parallel, to calculate the percentage of viable cells in the population. Viability was determined in plating assays on YPD. Bars correspond to the mean (plus SD) of three independent experiments. (C) Percentage of viable cells in cultures of wild type, *Δgrx1/2*, *Δgrx1/2 GRX7** or *Δgrx1/2 GRX1* (strain MML1152) cells after 12 hours of selenite treatment, made relative to viability of wild type cells (100%). Bars represent the mean (plus SD) of three independent experiments.

Fig. 3. Effect of 6 mM sodium selenite (added at time 0 at a culture concentration of 10^7 cells/ml) on the percentage of membrane-compromised cells (stained by methylene blue) in cultures of wild type cells (W303-1A), mutant *Δgrx1/2* cells (MML752) or mutant cells expressing the truncated form of Grx7p (*Δgrx1/2 GRX7**, MML1051), in YPD medium at 30ºC. Cultures were diluted with fresh medium without or with selenite when they reached a concentration of 3-4x10^7 cells ml^{-1}. Microscopy analyses were done when cultures were at a concentration of 1-2x10^7 cells ml^{-1}. Bar values are the mean (plus SD) of at least three independent experiments.

Fig. 4. Effect of sodium selenite on the appearance of apoptotic markers in cultures of wild type cells (W303-1A), mutant *Δgrx1/2* cells (MML752) or mutant cells expressing the truncated form of Grx7p (*Δgrx1/2 GRX7**, MML1051), in YPD medium at 30ºC. Conditions of treatment and dilution with prewarmed medium were as indicated in Methods and legend of Fig. 2. (A) DAPI staining of nuclei of wild type cells at the indicated times after addition of 6 mM sodium selenite at time 0 (upper panels). Lower panels correspond to the corresponding phase contrast images. (B) TUNEL staining (left panels) and the corresponding phase contrast (right panels) images of wild type cells treated with 6 mM sodium selenite for the indicated times. (C) Percentage of TUNEL-positive cells in cultures of the indicated strains after different times of 6 mM sodium selenite treatment. Bar values are the mean (plus SD) of at least three independent experiments. (D) Percentage of TUNEL-positive (black bars) and methylene blue-permeable (white bars) cells in cultures of wild type cells treated for 24 hours with 3 mM or 4 mM sodium selenite. Bar values are the mean (plus SD) of three independent experiments.

Fig. 5. Selenite-induced apoptosis in *S. cerevisiae* and mitochondrial functions. (A) Percentage of TUNEL-positive cells after 24 hours of 6 mM sodium selenite treatment in YPD medium at 30ºC. Cultures of wild type cells (W303-1A) and the following mutants were analyzed: MML1166 (*Δaif1*), MML1165 (*Δndi1*), MML1167 (*Δcox12*), MML1133 (*Δyca1*). Conditions of treatment and dilution with prewarmed medium were as indicated in Methods and legend of Fig. 2. Bar values are the mean (plus SD) of three independent experiments. (B) Cell viability in MML1166 (*Δaif1*) and W303-1A (wild type) cultures after different times of 6 mM sodium selenite treatment in YPD medium at 30ºC. The percentage of viable cells at each time point was calculated as described in Methods. Results are represented as the ratio between the viability index in the *Δaif1* and wild type cultures. Bar values are the mean (plus SD) of three

independent experiments. (C) Effect of sodium selenite at the indicated concentrations on wild type cells growing in YPGly medium at 30ºC. The following parameters were determined after 24 hours of treatment: relative total cell number (treated/untreated cultures), percentage of methylene blue-permeable cells and of TUNEL-positive cells. Bar values are the mean (plus SD) of three independent experiments.

Fig. 6. Accumulation of carbonylated proteins and ROS in cultures of wild type cells (W303-1A), mutant *Δgrx1/2* cells (MML752), mutant cells expressing the truncated form of Grx7p (*Δgrx1/2 GRX7**, MML1051), or *Δaif1* cells (MML1166). Initial conditions of treatment and dilution with prewarmed medium were as indicated in Methods and legend of Fig. 2. (A and B) Western blot analysis of protein carbonylation with anti-DNPH antibodies. Cell extracts were obtained from cultures of the indicated strains after different times of treatment with 6 mM (A) or 7 mM (B) sodium selenite in YPD medium at 30ºC. Each lane was loaded with 10 μg of protein. Numbers under each lane indicate the relative amount of protein (with respect to wild type cells at time 0), after scanning and densitometric quantification of the Coommassie Blue-stained blotted membranes. (C) Fluorescence emission rate by cells to which dihydroethidium had been added as described in Methods. Cell samples were taken from cultures at the indicated times of 6 mM selenite treatment. Values are made relative to the unit value corresponding to the fluorescence emission rate by wild type cells before selenite addition. Bars are the mean values (plus SD) of three independent experiments.

Fig. 7. Effect of sodium selenite on the appearance of canavanine-resistant mutants. (A) Wild type (CML235) and *Δgrx1 Δgrx2* (MML1178) cells growing exponentially in YPD medium were added at time 0 with 6 mM sodium selenite, and at the indicated times samples were taken to determine in parallel the concentration of viable cells and of canavanine-resistant (can^R) mutants. Initial conditions of treatment and dilution with prewarmed medium were as indicated in Methods and legend of Fig. 2. Bars represent the frequency of can^R mutants per 10^5 viable cells (mean plus SD, three independent experiments) (B) The same strains as above plus the MML1183 mutant (*Δgrx1 Δgrx2 GRX7**) were grown in YPD and treated for 12 and 18 hours with 6 mM sodium selenite, before determination of the concentration of viable cells and can^R mutants. Bars represent the frequency of can^R cells in the two mutant strains relative to the wild type strain (mean plus SD, three independent experiments).

(A)

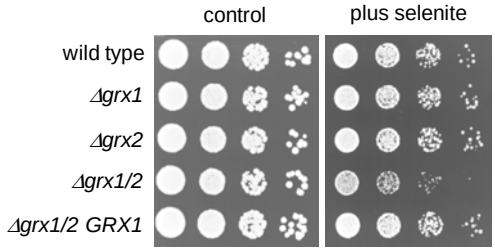
control
plus selenite
wild type
Δgrx1
Δgrx2
Δgrx1/2
Δgrx1/2 GRX1

(B)

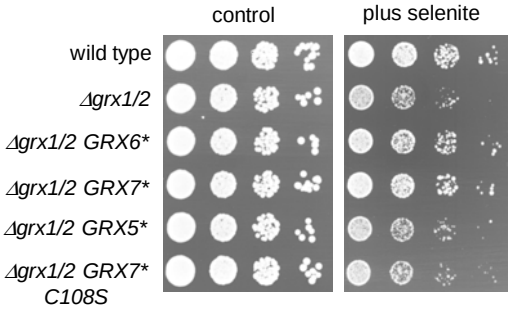
control
plus selenite
wild type
Δgrx1/2
Δgrx1/2 GRX6*
Δgrx1/2 GRX7*
Δgrx1/2 GRX5*
Δgrx1/2 GRX7* C108S

(C)

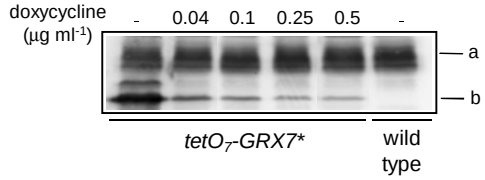
doxycycline (μg ml-1)
-
0.04
0.1
0.25
0.5
-
a
b
tetO7-GRX7*
wild type

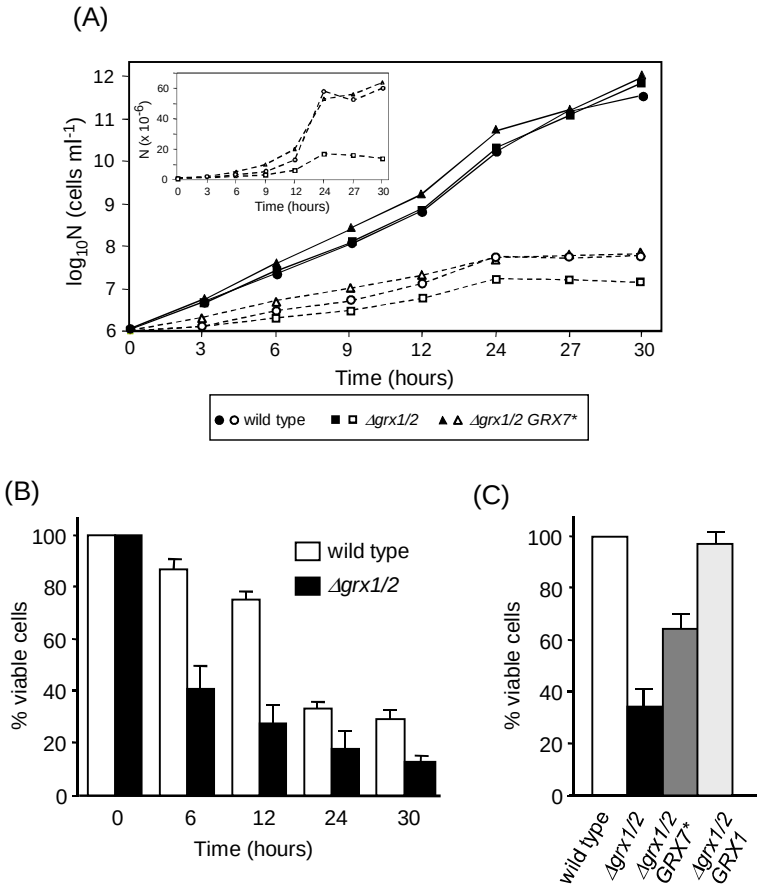
(A)
log10N (cells ml-1)
Time (hours)
N (x 10-6)
wild type
Δgrx1/2
Δgrx1/2 GRX7*
(B)
% viable cells
Time (hours)
wild type
Δgrx1/2
(C)
% viable cells
wild type
Δgrx1/2
Δgrx1/2 GRX7*
Δgrx1/2 GRX1

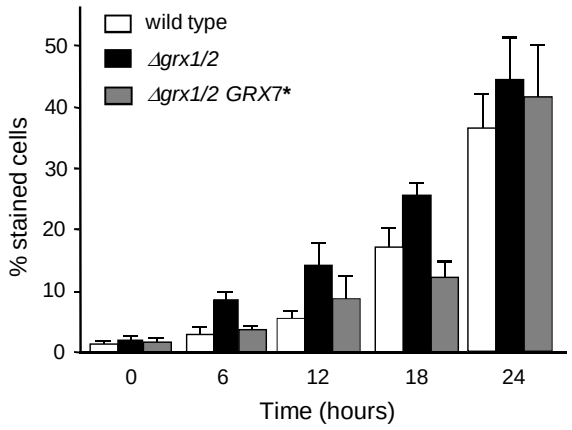
wild type
Δgrx1/2
Δgrx1/2 GRX7*
% stained cells
0
10
20
30
40
50
0
6
12
18
24
Time (hours)

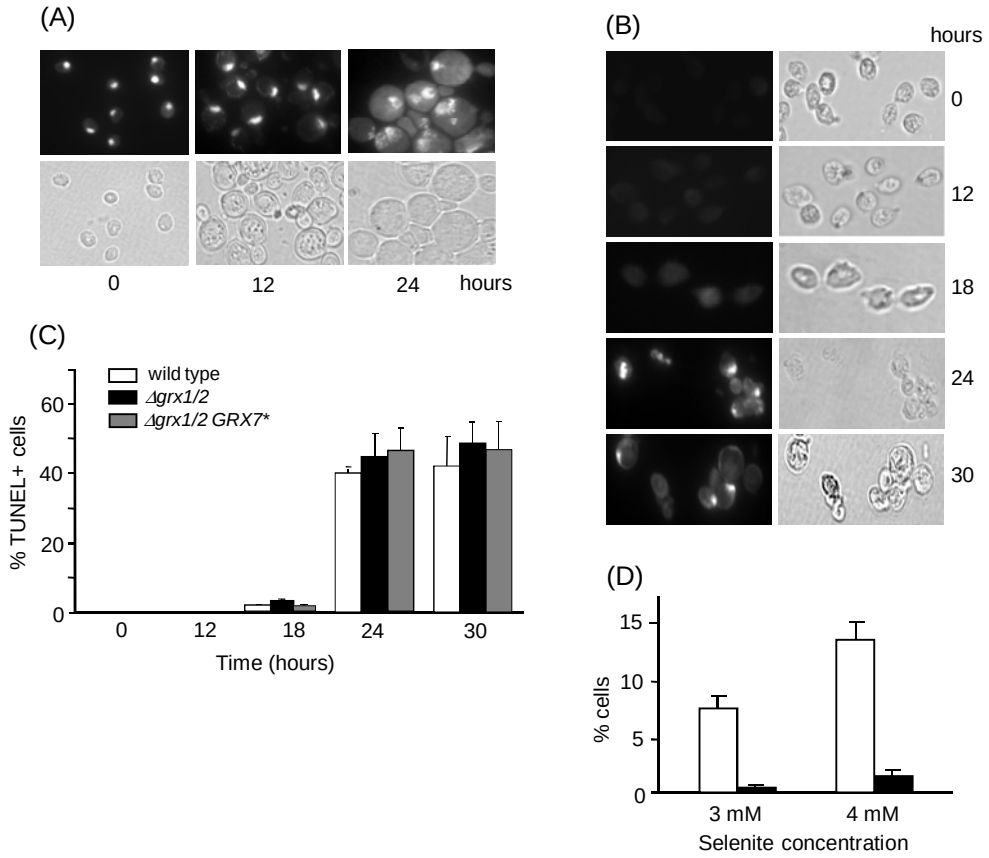
(A)
0
12
24
hours
(B)
hours
0
12
18
24
30
(C)
wild type
Δgrx1/2
Δgrx1/2 GRX7*
% TUNEL+ cells
60
40
20
0
0
12
18
24
30
Time (hours)
(D)
% cells
15
10
5
0
3 mM
4 mM
Selenite concentration

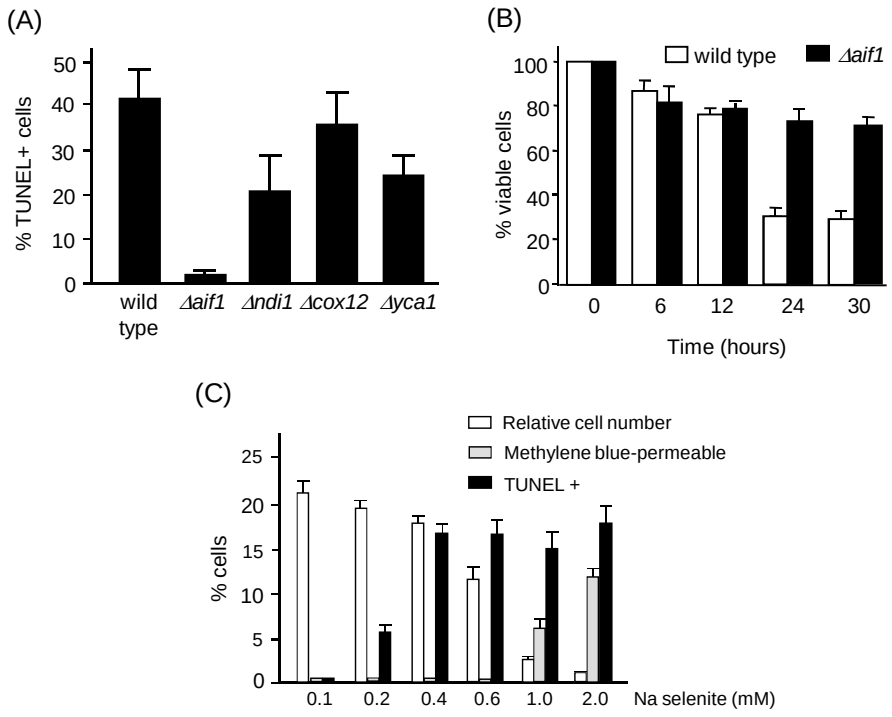
(A)
% TUNEL+ cells
50
40
30
20
10
0
wild type
Δaif1
Δndi1
Δcox12
Δyca1
(B)
wild type
Δaif1
% viable cells
100
80
60
40
20
0
0
6
12
24
30
Time (hours)
(C)
Relative cell number
Methylene blue-permeable
TUNEL +
% cells
25
20
15
10
5
0
0.1
0.2
0.4
0.6
1.0
2.0
Na selenite (mM)

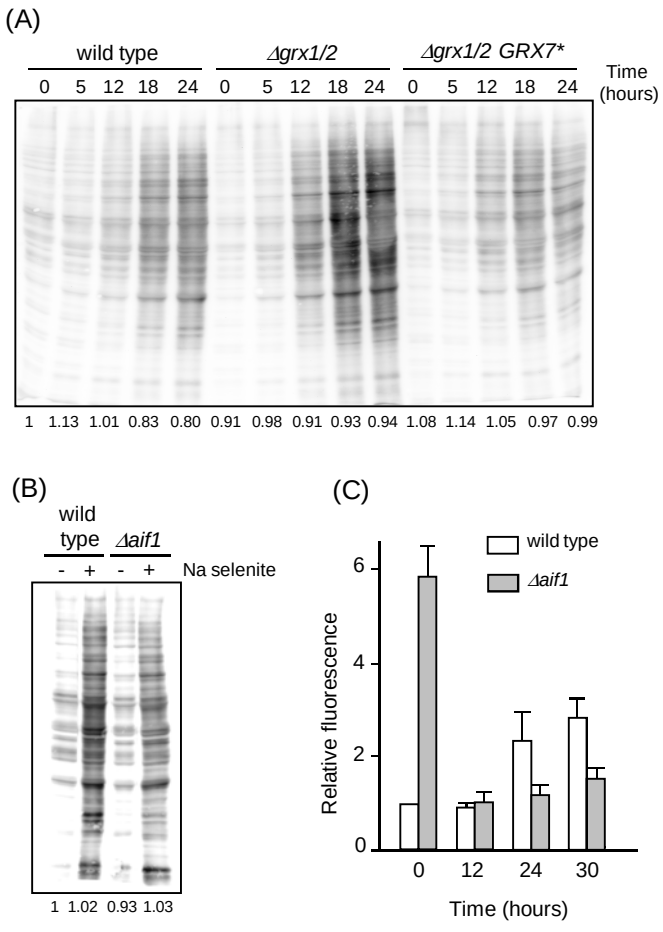
(A)
wild type
Δgrx1/2
Δgrx1/2 GRX7*
Time (hours)
0 5 12 18 24 0 5 12 18 24 0 5 12 18 24
1 1.13 1.01 0.83 0.80 0.91 0.98 0.91 0.93 0.94 1.08 1.14 1.05 0.97 0.99
(B)
wild type
Δaif1
- + - +
Na selenite
1 1.02 0.93 1.03
(C)
wild type
Δaif1
Relative fluorescence
0
2
4
6
0 12 24 30
Time (hours)

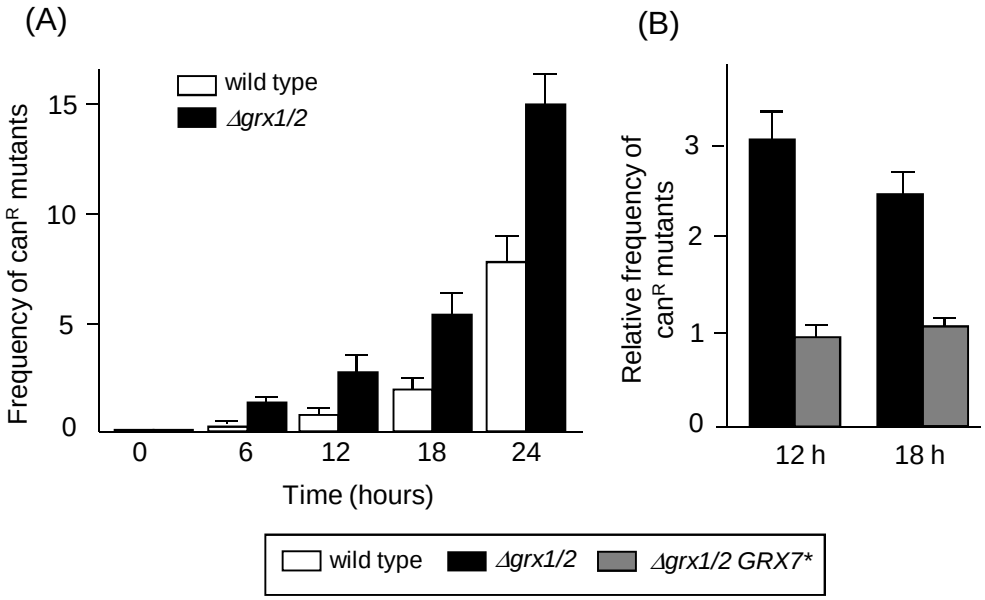
(A)
wild type
Δgrx1/2
Frequency of canR mutants
15
10
5
0
0
6
12
18
24
Time (hours)
(B)
Relative frequency of canR mutants
3
2
1
0
12 h
18 h
wild type
Δgrx1/2
Δgrx1/2 GRX7*